Proceedings of the International Conference on Oxide Materials for Electronic Engineering (OMEE 2021)

Eutectic Composites in Al_2O_3–Y_2O_3 System Solidified by Horizontal Directed Crystallization Method

Y. Siryk, O. Vovk*, L. Gryn, A. Romanenko, V. Baranov and S. Nizhankovskyi

Institute for Single Crystals, National Academy of Sciences of Ukraine, Nauky Ave. 60, Kharkiv, Ukraine

Doi: 10.12693/APhysPolA.141.268 *e-mail: oleh.vovk@isc.kharkov.ua

Al_2O_3–YAG eutectics bulk crystals have been obtained by the horizontal directional crystallization method under the total pressure of 1.3×10^5 Pa. Two approaches have been applied to reach the given morphology: (i) the first one consisted of the direct solidification of the melt of Al_2O_3 and Y_2O_3 to crystallize the Al_2O_3–YAG eutectics below 2000°C, (ii) the second one included two stages, i.e., the crystallization of the metastable eutectic Al_2O_3–YAP overheated to 2000°C followed by phase transformation from YAP to YAG at the evaluated temperature. The first approach resulted in the crystal with "Chinese script" morphology, which increased in the interphase segments with the lowering rate of crystallization. The morphology of the original Al_2O_3–YAP eutectic is tubular, but could be easily and quickly transformed into Al_2O_3–YAG "Chinese script" at 1700°C keeping the dimensional structure of the Al_2O_3–YAP. The interphase segments in such eutectics were mostly fine among all samples produced and were equal to 1.7 μm for the Al_2O_3 phase and 2.9 μm for the YAG phase. As a result, it has been shown that the horizontal directional crystallization method is applicable to the production of eutectics of Al_2O_3–YAG with a controlled structure. Such eutectics can be used at high temperatures as construction materials and as optical media with high scattering features.

topics: eutectics Al_2O_3–YAG, horizontal directional crystallization, interphase distance

1. Introduction

Eutectics of sapphire with yttrium aluminium garnet, Al_2O_3–$Y_3Al_5O_{12}$ (YAG), are intensively investigated as materials for applications at high temperatures due to excellent high-temperature strength characteristics, creep resistance, superior oxidation resistance and thermal stability in the ambient atmosphere at very high temperatures [1–5]. Recently, materials based on this eutectics have gained interest as optical media for light converters in modern solid-state luminaries with lasers as a primary light source, i.e., laser diode-based solid-state lightning (LD SSL). Such media must have high thermal conductivity and effectively scatter the laser beam to enhance light harvesting [6]. The eutectics of Al_2O_3–YAG are produced by laser floating zone [7], micro pulling down technique [8], optical floating zone methods [9], edge defined film growth technique [10], and the Bridgman technique [11]. Usually, the morphology of these eutectics resembles "Chinese script", which determines the mechanical and scattering properties at interphase distances, while lowering the interphase distances enhances the properties. Growth techniques with high gradients and rates of solidification allow the production of eutectics with tiny morphology, but the size of the crystal limits their practice usage. Applying the horizontal directional solidification with a relatively slow rate and low solidification gradient allows the vacuum growth of the bulk eutectics crystals with the interphase distances of 3.1 ± 1.8 μm [12].

Another way to produce eutectics of Al_2O_3–YAG of fine morphology is the phase transformation of the perovskite $YAlO_3$ (YAP) into the garnet YAG. According to the phase diagram of the Al_2O_3–Y_2O_3 system [13], among the Al_2O_3–YAG eutectics in this system there is a metastable Al_2O_3–YAP eutectic, which solidifies below 1700°C at a high rate of crystallization or solidifies from the melt overheating above 2000°C. These metastable eutectics can be transformed into Al_2O_3–YAG by heating the crystals beyond the melting temperature of the Al_2O_3–YAP eutectics of 1700°C. According to the reaction

$$Al_2O_3 + 3AlYO_3 = Y_3Al_5O_{12} \qquad (1)$$

The transformation occurs so easily and quickly that the crystal morphology changes while keeping the dimensional characteristics of the crystal segments. However, the disadvantage of this transformation according to reaction (1) is the expansion of the crystal volume by 11% [14], which could cause cracks in the crystals.

In the present work, the composites solidified in the Al_2O_3-Y_2O_3 system have been investigated in order to determine the conditions for obtaining the Al_2O_3–YAG eutectic with a given morphology by the horizontal directional crystallization method. A gas environment was applied instead of the vacuum. Two approaches have been studied to reach a given morphology, first is the direct solidification of the melt of Al_2O_3 and Y_2O_3 to crystallize the Al_2O_3–YAG eutectics, and the second one included two stages, i.e., the crystallization of the metastable eutectic of Al_2O_3–YAP followed by phase transformation on YAP into YAG at the evaluated temperature.

2. Experimental

The tablets of the mixture of 81.5 mol.% Al_2O_3 (99.999%) and 18.5 mol.% Y_2O_3 (99.999%) have been air annealed under 1200°C for 2 h and were applied as raw materials. The "Horizont-3" installation (Ukraine) was used for crystal growth by the horizontal directional crystallization method (HDC) in Mo crucible under the environment of Ar, CO, and H_2 at a total pressure of 1.3×10^5 Pa at the evaluated temperature and a given rate of solidification. Details of the installation scheme and solidification process are described in [15].

Examination of the samples cut out from the crystals were carried out with a scanning electron microscopy (SEM) using the JEOL JSM-6390LV microscope and energy-dispersive X-ray spectroscopy (EDS) using the silicon drift detector (SSD) by X-MaxN Oxford Instruments. XRD patterns of crystal phases that compose the crystals were established with a powder XRD diffractometer "DRON-3". The interphase distances in the eutectics structure were estimated using a specially developed procedure.

3. Results and discussion

3.1. Phase composition and morphology of directly solidified crystals

Crystals with a composition corresponding to eutectics of Al_2O_3–YAG in the Al_2O_3-Y_2O_3 system have been grown with different rates of solidification and initial temperature of the melt. A typical image of the crystal is shown in Fig. 1. The characteristic feature observed in the image is the presence of blocks elongated in the growth direction. The growth rate, the initial temperature of the melt, and the phase composition of the crystals are given in Table I.

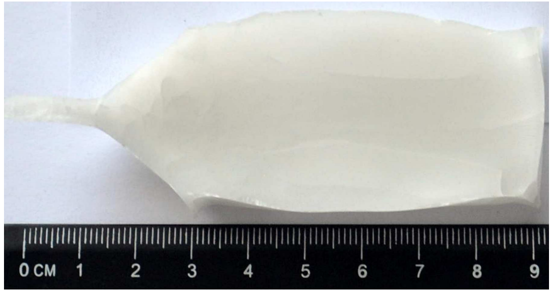

Fig. 1. General view of Al_2O_3–YAG eutectic crystal grown by HDC.

TABLE I

Growth rate, melt temperature, and eutectics phases of the crystals.

Sample (crystal)	Growth rate [mm/h]	Melt temperature [°C]	Eutectic phases
1	50	1925	Al_2O_3-$Y_3Al_5O_{12}$
2	30	1915	Al_2O_3-$Y_3Al_5O_{12}$
3	15	1985	Al_2O_3-$Y_3Al_5O_{12}$
4	5	1900	Al_2O_3-$YAlO_3$

Two compositions of crystal phases has been revealed, i.e., the eutectics of sapphire with garnet — Al_2O_3–YAG, and the eutectics of sapphire with perovskite — Al_2O_3-YAP. The appearance of these compositions of the crystals was not affected by the growth rate but was dependent on the temperature of the initial melt. The phase of perovskite YAP in eutectics with Al_2O_3 is formed instead of garnet phase YAG when the initial melt temperature reaches about 2000°C, which agrees with the previous study by Yasuda et al. [16].

Figure 2 shows the morphology of the eutectics crystals grown under the different rates of solidification of 5, 30, and 50 mm/h. All crystals were solidified at a temperature far below 2000°C. The composition of the crystals consists of the YAG and Al_2O_3 phase only (see the XRD pattern in Fig. 3b, d, and g). The morphology motif of the crystals is like the "Chinese script" and similar for all crystals, but the inter-phase distances are quite different. The inter-phase distances are not strictly defined in "Chinese script" morphology in contrast to laminar eutectics structures. But one can see that it is fine for the crystal grown at the solidification rate of 50 mm/h and becomes coarser when the rate is lowered.

We developed a technique to estimate the interphase structure in the eutectics with "Chinese script" morphology and to be able to compare the morphology of such eutectics crystals. This technique is based on linear scanning of an image of the eutectics surface and measuring the length of the segments that resulted in crossing the inter-phase. After that, the dependence the number of segments of defined size with specified tolerance from

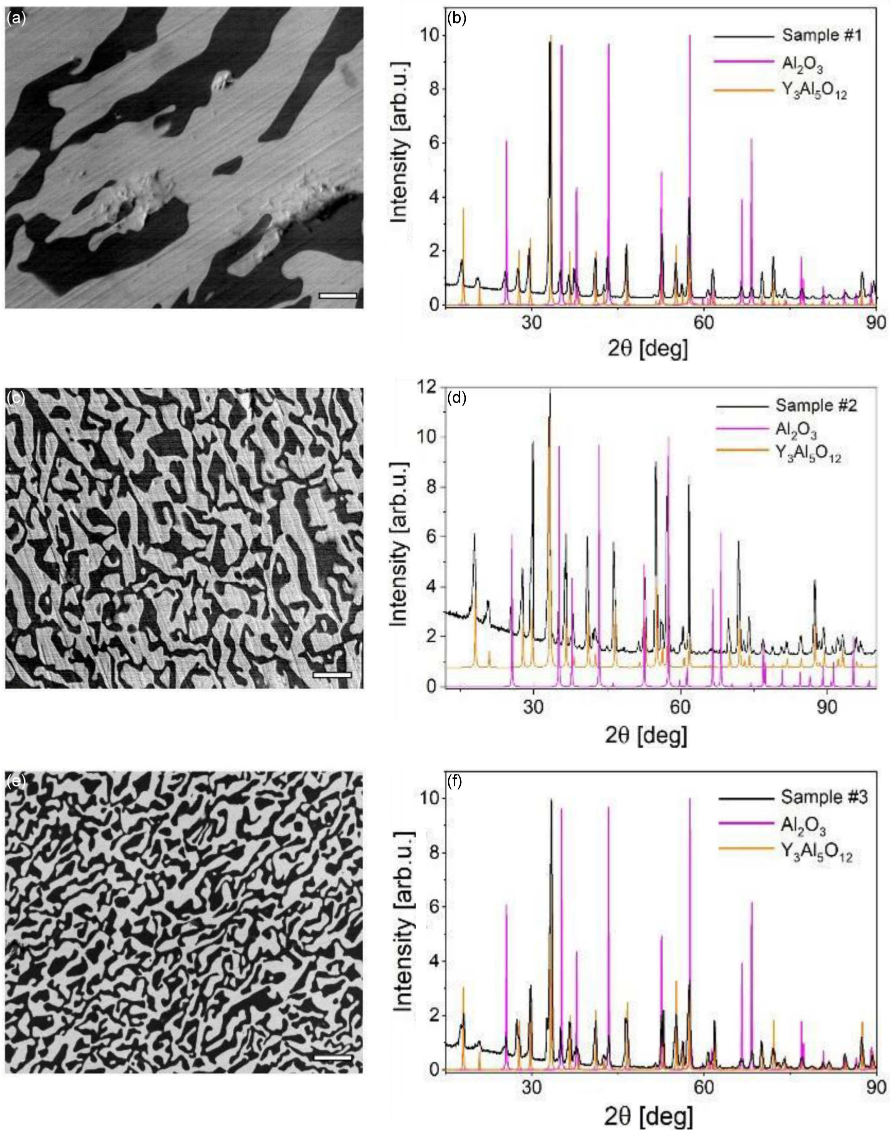

Fig. 2. SEM images and XRD patterns of the samples grown at crystallization rates of 5 (a, b), 30 (c, d), and 50 mm/h (e, f). The scale bar is 10 μm, the dark phase — Al_2O_3, the light phase — YAG.

the average segment size was built. This technique is sensitive to the texture of the image. To reveal the texture, the image should be scanned in different directions. No differences in segment distribution were revealed for all samples scanned at different angles.

In Fig. 3, the relative distribution n/N of the length d of the cross-section segments for sapphire (Al_2O_3) (a) and YAG (b) phases are shown, where n is the number of cross-sectional segments of length d, N is the total number of cross-sectional segments of the phase studied on the SEM image of the microstructure. The eutectics solidified at 5 mm/h possess a wide distribution of segments with several local maxima, while the eutectics grown at 30 and 50 mm/h are characterized by a distribution with one maximum. The average size of the YAG segments is strongly dependent on the rate of solidification, more so than the segments of the sapphire phase. On the visual view, the morphology of sample 2 looks coarser than sample 1, although the average size of segments does not differ significantly. It could be explained by the small local maxima in the vicinity of 13 and 17 μm for both phases. The average size of segments of both phases is presented in Table II.

TABLE II

Growth rate and the average size of the segment for Al_2O_3 and YAG (YAP) phases.

Sample (crystal)	Growth rate [mm/h]	Average size of segment Al_2O_3 phase [μm]	Average size of segment YAG phase [μm]
1	50	3.9	3.7
2	30	4.1	5.1
3	15	1.7	2.9
4	5	13.4	22.5

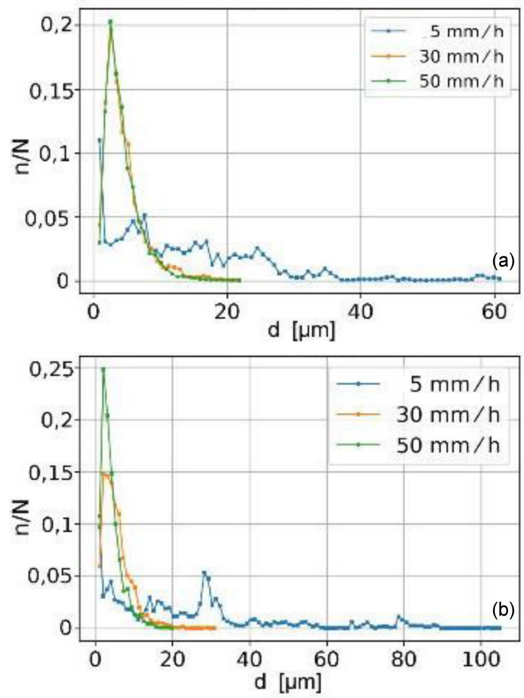

Fig. 3. Relative distribution n/N of the length d of the cross-section segments for the phases of sapphire (a), and YAG (b) in Al_2O_3–YAG grown at 5, 30, and 50 mm/h, where d is the length of the cross-sectional segment, n is the number of cross-sectional segments of length d, N is the total number of cross-sectional segments of the phase studied on the SEM images.

3.2. Morphology and phase composition of the crystals after phase transformation

Crystal 3 has been solidified at a temperature near 2000°C, and its morphology looks like a tubular structure and strongly differs from the morphology of the Al_2O_3–YAG eutectics (see Fig. 4a). This crystal is composed of Al_2O_3-YAP eutectics according to the XRD pattern (see Fig. 4b), with an average size of YAP segments of 2.9 μm and Al_2O_3 segments of 1.7 μm (see Table II). It should be noted that is smaller than the one in the samples of Al_2O3-YAG eutectics, and the growth conditions in its case are more convenient for the technological route.

The sample prepared from crystal 3 has been transformed into the Al_2O_3–YAG composition by heating to the temperature of 1860°C, which is higher than the melting point of the Al_2O_3–YAG ceramics. The phase composition consists only of Al_2O_3 and YAG, which has been proven by the XRD pattern shown in Fig. 4d. The morphological motif of the crystals changes from tubular to a "Chinese script", but the dimension of the structural segments remains as in Al_2O3–YAP systems, which is lower than in the sample directly solidified even at the high rate, i.e., 50 mm/h. No cracks have appeared in the samples after YAP to YAG transformation, which is a promising result for obtaining bulk crystals of Al_2O_3–YAG eutectics with tiny segmental structures. Such materials can compete with single crystals and Al_2O_3–YAG ceramics in high-temperature applications and scattering media for LD SSL.

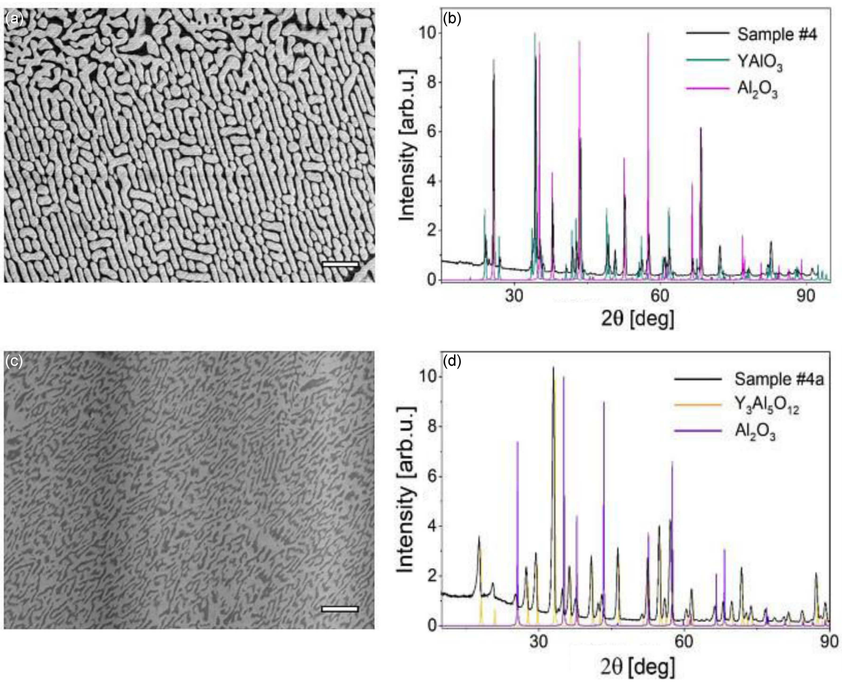

Fig. 4. SEM images and XRD patterns of Al_2O_3-YAP metastable eutectic (a, b) and the same sample after transformation into Al_2O_3–YAG eutectics (c, d). The scale bar is 10 μm, the dark phase — Al_2O_3, the light phase — YAG/YAP.

4. Conclusions

The Al_2O_3–YAG eutectics bulk crystals have been obtained by the HDC method under the total pressure of 1.3×10^5 Pa. Using pressure slightly higher than the ambient pressure instead of a vacuum has some advantages in the technological route of HDC. The morphology of these eutectics is like "Chinese script" with roughness depending on the rate of solidification. Lowering of this rate causes an increase in the interphase distances. The finest interphase morphology was obtained as a result of the transformation of metastable eutectics Al_2O_3–YAP into Al_2O_3–YAG. Moreover, the original Al_2O_3–YAP eutectics were obtained by the most convenient technological route.

As a result, it has been shown that the HDC method is applicable to the production of eutectics of Al_2O_3–YAG with a controllable structure. Such eutectics can be used at high temperatures as construction materials and as optical media with high scattering features.

Acknowledgments

This work has been done in the framework of the project No. 84/DTF-2SC-26/20-22 "Physical and technological bases for the creation of luminescent crystalline composites for powerful LED/LD white lighting" of the National Academy of Sciences of Ukraine.

References

[1] T. Man, T.A. Rathasaratha, L.E. Matson, *Ceram. Eng. Sci. Proc.* **11**, 1617 (1990).

[2] J. Zhang, H. Su, K. Song, L. Liu, H. Fu, *J. Eur. Ceram. Soc.* **31**, 1191 (2011).

[3] Y. Waku, N. Nakagawa, T. Wakamoto, H. Ohtsubo, K. Shimizu, Y. Waku, *J. Mater. Sci.* **33**, 1217 (1998).

[4] N. Nakagawa, H. Ohtsubo, A. Mitani, K. Shimizu, Y. Waku, *J. Eur. Ceram. Soc.* **25**, 1251 (2005).

[5] Y. Waku, N. Nakagawa, H. Ohtsubo, A. Mitani, K. Shimizu, *J. Mater. Sci.* **36**, 1585 (2001).

[6] S. Li, L. Wang, N. Hirosaki, R. Xie, *Laser Photonics Rev.* **12**, 1800173 (2018).

[7] M.C. Mesa, P.B. Oliete, V.M. Orera, J.Y. Pastor, A. Martín, J. LLorca, *J. Eur. Ceram. Soc.* **31**, 1241 (2011).

[8] B.M. Epelbaum, A. Yoshikawa, K. Shimamura, T. Fukuda, K. Suzuki, Y. Waku, *J. Cryst. Growth* **198-199**, 471 (1999).

[9] X. Wang, Y. Zhong, D. Wang, L. Sun, B. Jiang, J. Wang, *J. Am. Ceram. Soc.* **101**, 1029 (2018).

[10] L.E. Matson, N. Hecht, *J. Eur. Ceram. Soc.* **19,** 2487 (1999).

[11] X. Wang, W. Zhang, Q. Xian, J. Shen, G. Zhang, D. Wang, J. Wang, L. Lou, J. Zhang, *J. Eur. Ceram. Soc.* **38**, 5625 (2018).

[12] Y. Nie, M. Zhang, Y. Liu, Y. Zhao, *J. Alloys Compd.* **657**, 184 (2016).

[13] J.L. Caslavsky, D.J. Viechnicki, *J. Mater. Sci.* **15**, 1709 (1980).

[14] T. Nagira, H. Yasuda, T. Sakimura, K. Yoshida, *J. Eur. Ceram. Soc.* **32**, 2137 (2012).

[15] S.V. Nizhankovskyi, A.V. Tan'ko, Yu.N. Savvin, S.I. Krivonogov, A.T. Budnikov, A.V. Voloshin, *Opt. Spectrosc.* **120**, 915 (2016).

[16] H. Yasuda, I. Ohnaka, Y. Mizutani, Y. Waku, *Sci. Technol. Adv. Mater.* **2**, 67 (2001).